Liquid Crystals
Publication details, including instructions for authors and subscription information:
http://www.informaworld.com/smpp/title~content=t713926090

Self-assembly of a coil-rod-coil block molecule complexed with $LiCF_3SO_3$

Yoon-Sok Kang[a]; Wang-Cheol Zin[a]; Dong-Woo Lee[b]; Myongsoo Lee[b]
[a] Polymer Research Institute and Department of Materials Science and Engineering, Pohang University of Science and Technology, Pohang 790-784, Korea, [b] Department of Chemistry, Yonsei University, Shinchon 134, Seoul 120-749, Korea,

To cite this Article Kang, Yoon-Sok , Zin, Wang-Cheol , Lee, Dong-Woo and Lee, Myongsoo(2000) 'Self-assembly of a coil-rod-coil block molecule complexed with $LiCF_3SO_3$', Liquid Crystals, 27: 11, 1543 — 1550
To link to this Article: DOI: 10.1080/026782900750018726
URL: http://dx.doi.org/10.1080/026782900750018726

LIQUID CRYSTALS, 2000, VOL. 27, NO. 11, 1543–1550

Self-assembly of a coil–rod–coil block molecule complexed with $LiCF_3SO_3$

YOON-SOK KANG, WANG-CHEOL ZIN*

Polymer Research Institute and Department of Materials Science and Engineering,
Pohang University of Science and Technology, Pohang 790-784, Korea

DONG-WOO LEE and MYONGSOO LEE

Department of Chemistry, Yonsei University, Shinchon 134, Seoul 120-749, Korea

(*Received 16 February 2000; accepted 25 May 2000*)

Enantiotropic liquid crystalline phases were induced by the complexation of docosyl 4-(4-oxy-4′-biphenylcarbonyloxy)-4′-biphenyl carboxylate, containing poly(ethylene oxide) of twelve ethylene oxide subunits, with 0.25 mol of $LiCF_3SO_3$ per ethylene oxide unit. The existence of oblique columnar, rectangular columnar (Col_{rec}), and smectic A (SmA) mesophases of this complex was demonstrated by a combination of polarized optical microscopy and X-ray diffraction. This complex was observed to transform from the rectangular columnar phase to a lamellar phase on heating. The unusual phase transition behaviour in this complex is believed to originate from the mixing entropy of the added $LiCF_3SO_3$. Also, the Col_{rec}–SmA phase transition was accompanied by a change of the packing structure from bilayer to monolayer.

1. Introduction

Scientific interest in the mesomorphic properties of rod–coil molecules has been growing rapidly in recent years due to their fascinating phase behaviour [1]. Rod–coil molecules consisting of a rigid rod block and a flexible coil block represent a novel class of self-assembling materials, since such molecules share general characteristics of both block copolymers and rod-like liquid crystalline molecules. Poly(hexyl isocyanate-*b*-styrene) rod–coil diblock copolymers have been reported to exhibit various unusual lamellar structures [2], while other rod–coil triblock systems have been reported to generate mushroom-like supramolecular assemblies [3]. It has been shown that diblock rod–coil molecules self-assemble into layered smectic, bicontinuous cubic, and hexagonal columnar structures depending on the relative length of the coil segment to the rod segment [4 *a*, *b*]. It has also been shown that coil–rod–coil triblock molecules self-assemble into discrete spherical micellar aggregates in the melt [4 *c*]. These interesting supramolecular assemblies are believed to arise from the competition between microphase separation of the rod and coil blocks into nanoscopically ordered periodic structures, and the tendency of the rod blocks to form anisotropic, orientationally ordered structures.

Poly(alkylene oxide), due to its complexation capability with alkali metal cations, can provide an application potential for solid polyelectrolytes and induce various liquid crystalline supramolecular structures. Poly(ethylene oxide) with flexible side groups induces a smectic A mesophase upon complexation with $LiClO_4$ [5 *a*], while the complexation of taper-shaped molecules containing oligo(ethylene oxide) with alkali metal trifluoromethanesulfonate induces a hexagonal columnar mesophase [5 *b*]. It has also been shown that control of the supramolecular structure in rod–coil molecular systems containing poly(alkylene oxide) from lamellar, to cubic, to cylindrical phases is possible through complexation with lithium ion [6].

We recently reported that the complexation of docosyl 4-(4-oxy-4′-biphenylcarbonyloxy)-4′-biphenyl carboxylate attached to poly(ethylene oxide) with twelve ethylene oxide subunits (E-12-22) with lithium trifluoromethanesulfonate (triflate) leads to columnar and smectic A mesophases [7]. The purpose of the work described in this paper is to elucidate the molecular packing structure of these liquid crystalline phases in detail and to understand the phase transition behaviour of pure and complexed E-12-22.

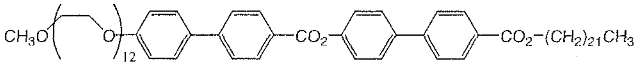

E-12-22

---

*Author for correspondence; e-mail: wczin@postech.ac.kr

Liquid Crystals ISSN 0267-8292 print/ISSN 1366-5855 online © 2000 Taylor & Francis Ltd
http://www.tandf.co.uk/journals

2. Experimental

Details of the synthesis of E-12-22 and its complexation with $LiCF_3SO_3$ are reported elsewhere [7]. The complex with 0.25 mol of $LiCF_3SO_3$ per ethylene oxide unit of E-12-22 is designated as E-12-22-0.25. A Perkin Elmer DSC-7 differential scanning calorimeter was used to determine the thermal transitions, with heating and cooling rates of 10°C min^{-1}. A Nikon Optiphot 2-pol polarized optical microscope (magnification: 100×) equipped with a Mettler FP 82 hot-stage and a Mettler FP 90 central processor was used to analyse the anisotropic texture. X-ray diffractograms were obtained with synchrotron radiation at the 3C2 and 4C2 X-ray beam line ($\lambda = 0.1608$ nm) at Pohang Accelerator Laboratory, Korea. *In situ* X-ray measurements were performed in transmission mode at various temperatures. The sample holder was heated with two cartridge heaters, and the temperature was monitored. A 7 µm thick Kapton film window was used to contain the samples in the fluid liquid crystalline states, and the scattered intensity from the Kapton window was subtracted.

3. Results and discussion

3.1. *Crystalline state*

The ABC coil–rod–coil triblock molecule (designated as ABC triblock molecule) used in this research consists of three parts: poly(ethylene oxide) as the A block, a molecular rod consisting of two biphenyl units as the B block, and docosyl as the C block. Owing to the microphase segregation tendency of each block, pure and complexed ABC triblock molecules are expected to form a self-assembled structure in their crystalline and liquid crystalline states.

Figure 1 displays the X-ray diffraction (XRD) patterns of pure and complexed ABC triblock molecules obtained at 70°C. Figure 1 (*a*) shows three Bragg reflections at reciprocal space ratios of 1 : 2 : 3, and figure 1 (*b*) displays two Bragg reflections at reciprocal space ratios of 1 : 2 in the small angle region. These ratios, together with sharp reflections in the wide angle region as shown in figures 1 (*c*) and 1 (*d*), indicate that E-12-22 and E-12-22-0.25 are lamellar crystals below the melting temperature of the rod. The layer spacings of pure and $LiCF_3SO_3$-complexed ABC triblock molecules are 15.2 and 15.9 nm, respectively. The length of the E-12-22 molecule in its most extended conformation was calculated to be 9.5 nm, thus both pure and complexed E-12-22 are bilayered lamellar structures in their crystalline states.

At room temperature, added lithium triflate does not fully mix with poly(ethylene oxide), so peaks for the insoluble salt could be observed in the XRD profiles. These peaks disappeared above the melting temperature of the poly(ethylene oxide) segment because the insoluble salt can form a complex with the A block. In addition, the crystalline melting transitions of the ABC triblock molecule appear to have little dependence on the salt concentration [7]. Thus, the added lithium triflate is assumed to be selectively dissolved in the microphase-segregated poly(ethylene oxide) coil segments.

Figure 1 (*a*) shows that the second XRD peak, of the lamellar structure of the pure ABC triblock molecule is larger than first peak, whereas figure 1 (*b*) shows that the second peak in the lamellar morphology is smaller than first peak in E-12-22-0.25. The relative intensity of the XRD peak of successive order *n* in the lamellar structure depends not only upon the volume fraction of each

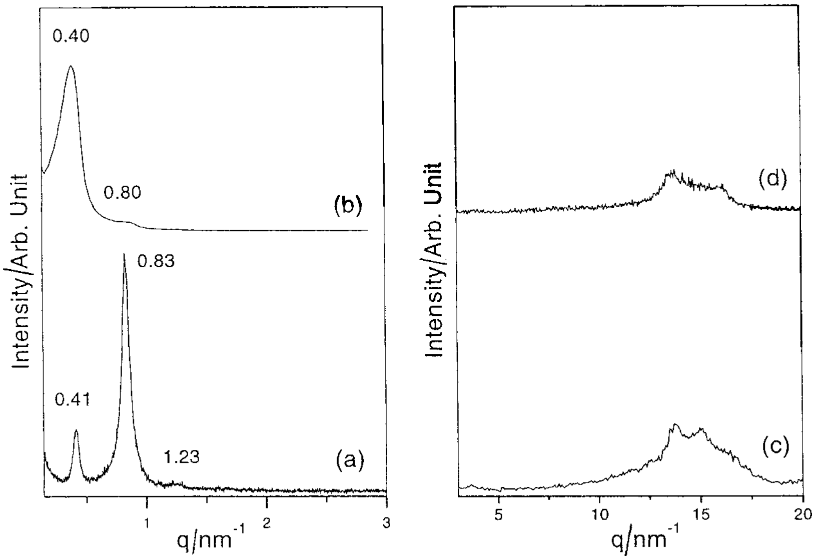

Figure 1. X-ray diffractograms of E-12-22 and E-12-22-0.25 at 70°C. Small angle X-ray diffraction patterns of (*a*) E-12-22 and (*b*) E-12-22-0.25; wide angle X-ray diffraction patterns of (*c*) E-12-22 and (*d*) E-12-22-0.25.

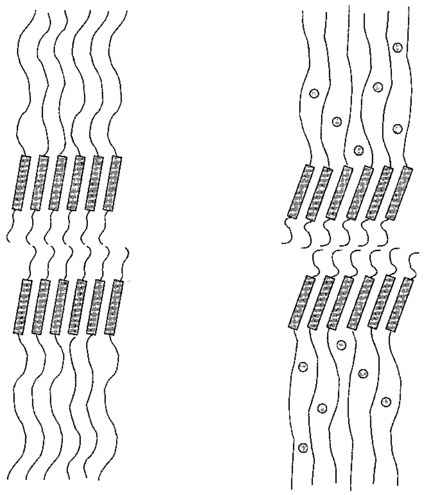
(a) (b)

Figure 2. Schematic representation of the packing structure of (*a*) E-12-22 and (*b*) E-12-22-0.25 in their crystalline state.

block but also upon the electron density of each part [8]†. Thus selective addition of lithium triflate to the poly(ethylene oxide) block results in a significant change of the relative heights of successive peaks.

The layer spacing of the ABC triblock molecule does not significantly increase by complexation (15.2→15.9 nm). From this it may be implied that the volume increment of the poly(ethylene oxide) domain, by complexation with $LiCF_3SO_3$, accompanies the tilt of ABC triblock molecule, as shown in figure 2. The tilt increases the separation between grafting sites, thus reducing the entropy loss of the poly(ethylene oxide) chains [9].

Table 1. Thermal transitions of E-12-22 and E-12-22-0.25. Data obtained from heating scan.

Compound	Phase transitions in °C, and corresponding enthalpy changes (kJ mol^{-1})
E-12-22	Cr 99.7 (44.7) SmC 118.2 (4.2) I
E-12-22-0.25	Cr 74.5 (22.6) Col_{ob} 125.4 (0.69) Col_{rec} 188.9 (0.2) SmA 257.1 (0.6) I

3.2. *Liquid crystalline state*

E-12-22 and E-12-22-0.25 show enantiotropic liquid crystalline behaviour as revealed by DSC and polarizing optical microscopy (POM). The phases and transition temperatures of these compounds are summarized in table 1. E-12-22 exhibits only a smectic C liquid crystalline phase. On cooling from the isotropic liquid, mosaic texture was observed as shown in figure 3 (*a*). In contrast, the addition of 0.25 mol of $LiCF_3SO_3$ to E-12-22 induces the formation of columnar and SmA mesophases. Figure 3 (*b*) is a pseudo-focal-conic texture of E-12-22-0.25, which is characteristic of the columnar phase; figure 3 (*c*) is a focal-conic texture of the complex, which is characteristic of SmA phase. Upon heating, the transition from mesophase to isotropic liquid occurs at 118 and 257°C for E-12-22 and E-12-22-0.25, respectively. The increase in the isotropization temperature (T_i) by complexation will be discussed later.

To corroborate the molecular packing structure, the mesophases of pure and complexed ABC triblock molecules were investigated by XRD. Pure E-12-22 showed only a SmC liquid crystalline state. In this mesophase, the sharp reflections observed in its crystalline state disappeared and a diffuse halo was observed in the wide angle region, figure 4 (*b*), indicating the melting of the aromatic rod. Figure 4 (*a*) shows small angle XRD pattern measured at 110°C. The ratio of the positions of the two sharp peaks shows that E-12-22 exhibits a lamellar structure at its mesophase. This ABC coil–rod–coil triblock molecule consists of three distinct and incompatible parts: a flexible and hydrophilic chain, a rigid central part, and a flexible and lipophilic unit. The number of unfavourable contacts among hydrophilic and hydrophobic flexible chains and rigid rods decreases when microphase-segregated assemblies are formed. According to the model suggested by Halperin [9], the aggregated rods are expected to favour ordered packing with their long axes aligned. In this structure, the rods are aligned and their tips toe the basal planes to achieve the minimum surface free energy. When the melted chains grafted to the basal plane are long enough, the free energy induced by the chain elongation is so large that the rods tilt in order to increase the separation between grafting sites. The repeat layer spacing of the SmC phase of E-12-22 is 10.2 nm, whereas the length of E-12-22 in its most extended conformation amounts to 9.5 nm. So it could be concluded that the SmC phase of E-12-22 is a bilayered lamellar structure with molecules tilted with respect to the lamellar axis. A schematic representation for the organization of the lamellar mesophase can be constructed as shown in figure 5 (*a*).

In contrast to the phase behaviour of E-12-22, E-12-22-0.25 exhibits columnar and SmA mesophases before isotropization. On heating from its crystalline state, the sharp reflections of E-12-22-0.25 disappeared and a diffuse halo was visible in the wide angle region,

---

† The intensity of scattering is given by $I(q) = |F(q)|^2 |Z(q)|^2$, where $F(q)$ and $Z(q)$ are the Fourier transforms of $\rho_u(r)$ and $z(r)$, respectively. $\rho_u(r)$ is the scattering length density distribution associated with a unit cell in the structure, and $z(r)$ is the function describing the ordered arrangement of such unit cells. The structure factor $F(q)$ is governed by the atomic content (electron density and volume fraction of each block) of the unit cell only.

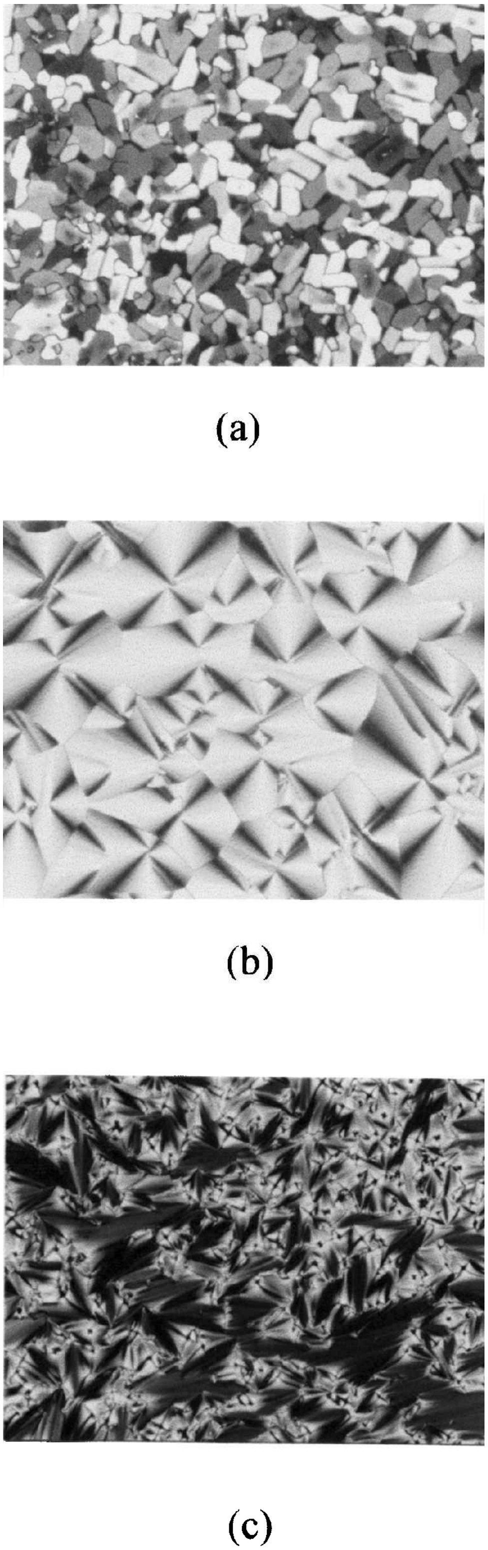

Figure 3. Representative polarized optical micrographs (100×) of the texture exhibited by (*a*) the smectic C mesophase of E-12-22 at 110°C on the cooling scan; (*b*) the columnar mesophase of E-12-22-0.25 at 170°C on the cooling scan; (*c*) the smectic A mesophase of E-12-22-0.25 at 225°C on the cooling scan.

figure 6 (*g*). The wide angle halo indicates a structure without long range order. Figure 6 (*b*) shows a number of sharp reflections in the small angle region. The peaks could be indexed on the basis of an oblique columnar (Col_{ob}) structure as summarized in table 2 [10, 11]. Upon heating, the transition from the oblique to the rectangular columnar phase occurs at 125°C. The peaks in the small angle region, figure 6 (*c*), could be assigned on the basis of a base-centred rectangular columnar 2D lattice (see table 2) [11–15]. A Col_{ob} and/or rectangular columnar (Col_{rec}) phase can be seen in other discotic liquid crystalline materials or polycatenar compounds [16, 17], but only a few examples of this mesophase formation by rod–coil molecules have been reported [18].

To describe the detailed supramolecular structure of the Col_{rec} phase, it is useful to calculate the number of molecules per cross-sectional slice of a column. From the measured Col_{rec} lattice constants (a, b) and the assumed density of $\rho = 1\ \mathrm{g\,cm^{-3}}$, the average number (n) of molecules per cross-sectional area of a cylinder can be estimated. Using equation (1), it can be calculated that about 37 molecules should be arranged in a cross-section of a column with a height (h) of 0.54 nm (estimated from the density of the rod blocks and the calculated length of a rod of 2.0 nm).

$$n = \frac{a \times b \times h \times 0.5 \times N_A \times \rho}{M} \tag{1}$$

(N_A: Avogadro's constant, M: sum of the molar mass of E-12-22 and complexed $LiCF_3SO_3$).

On the basis of the results obtained from XRD and the above calculation, a schematic representation of the organization of supramolecular cylinders into the rectangular columnar mesophase can be constructed as

Table 2. Detailed indexation of oblique (Col_{ob}) and base-centred rectangular (Col_{rec}) columnar phase of E-12-22-0.25.

Mesophase (lattice constants)	Reflections/nm		Miller indices (*h k l*)
	Measured	Calculated	
Col_{ob} at 108°C	22.66	22.64	(1 0 0)
$a = 22.77$ nm	11.64	11.64	(0 1 0)
$b = 11.70$ nm	10.80	10.80	(1-1 0)
$\gamma = 95.7°$	9.85	9.96	(1 1 0)
	8.55	8.56	(2-1 0)
Col_{rec} at 150°C	18.12	18.13	(2 0 0)
$a = 36.28$ nm	10.25	10.18	(1 1 0)
$b = 10.60$ nm	9.09	9.07	(4 0 0)
	7.95	7.97	(3 1 0)
	6.04	6.05	(6 0 0)
	5.30	5.30	(0 2 0)
	5.06	5.09	(2 2 0)

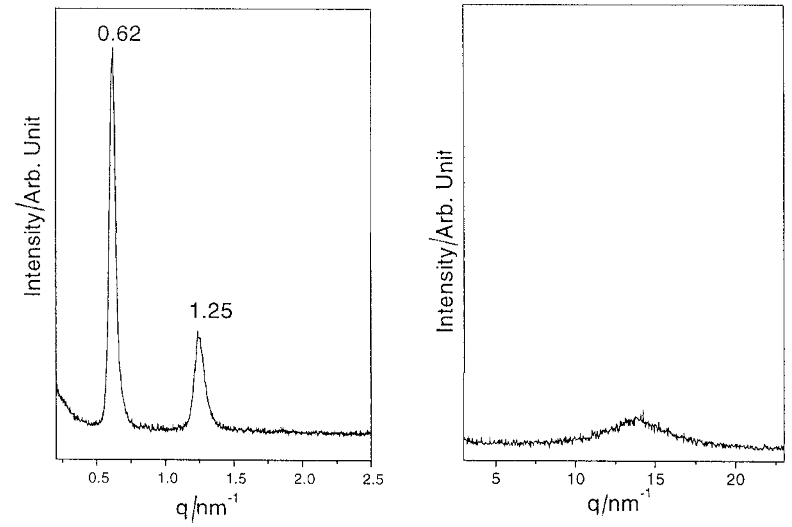

(a) (b)

Figure 4. X-ray diffraction patterns of E-12-22 at 110°C: (*a*) small angle XRD pattern, (*b*) wide angle XRD pattern.

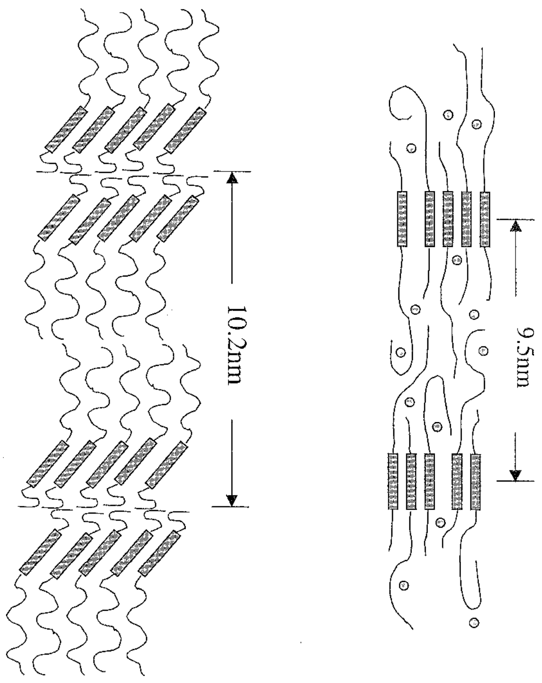

(a) (b)

Figure 5. Schematic representation of the structure of (*a*) E-12-22 in the SmC mesophase, (*b*) E-12-22-0.25 in the SmA mesophase.

shown in figure 7. Wide angle XRD also indicates a disordered arrangement of the molecules within a discrete aromatic core with rectangular cross-section, figure 6 (*h*). Although there is a broad amorphous halo in the wide angle XRD, the half-width Δq (scattering vector $q = 4\pi \sin \theta/\lambda$) of the wide angle halo increases from 3.7 nm^{-1} (Col$_{rec}$) to 4.9 nm^{-1} (isotropic). This result may suggest that there is ordering of the mesogens within the columns of the rectangular columnar liquid crystalline phase, as depicted in figure 7.

Figure 6 (*d*) shows the XRD pattern of E-12-22-0.25 obtained at 190°C; this pattern denotes the characteristic of a lamellar structure. Only a diffuse halo can be observed in the WAXS pattern, figure 6 (*i*), indicating that there are only weak liquid-like arrangements of the rods within the layer. These results together with POM confirm that E-12-22-0.25 displays a SmA mesophase with a lattice constant of 9.5 nm. The fully extended molecular length for the ABC triblock molecular is 9.5 nm. Since the effective volume of alkyl and poly(ethylene oxide) chains in the liquid crystalline state may be less than that of the rod unit length, the effective length for the ABC triblock molecule is less than 9.5 nm. The addition of lithium triflate may, however, increase the effective molecular length to 9.5 nm. So the complexed E-12-22-0.25 forms a monolayered lamellar structure as shown in figure 5 (*b*), whereas pure E-12-22 forms a bilayered lamellar structure, figure 5 (*a*).

E-12-22-0.25 undergoes isotropization at 257°C. In the isotropic phase only diffuse scattering is shown in the small angle region, because of the existence of density fluctuation in the triblock melt [19], figure 6 (*e*).

On cooling the isotropic phase, SmA and then the Col$_{rec}$, Col$_{ob}$ phases reappeared. The reappearance of the SmA, Col$_{rec}$ and Col$_{ob}$ morphology demonstrates that the transition is thermally reversible and hence that the phases exist in equilibrium at a certain temperature region in this complex.

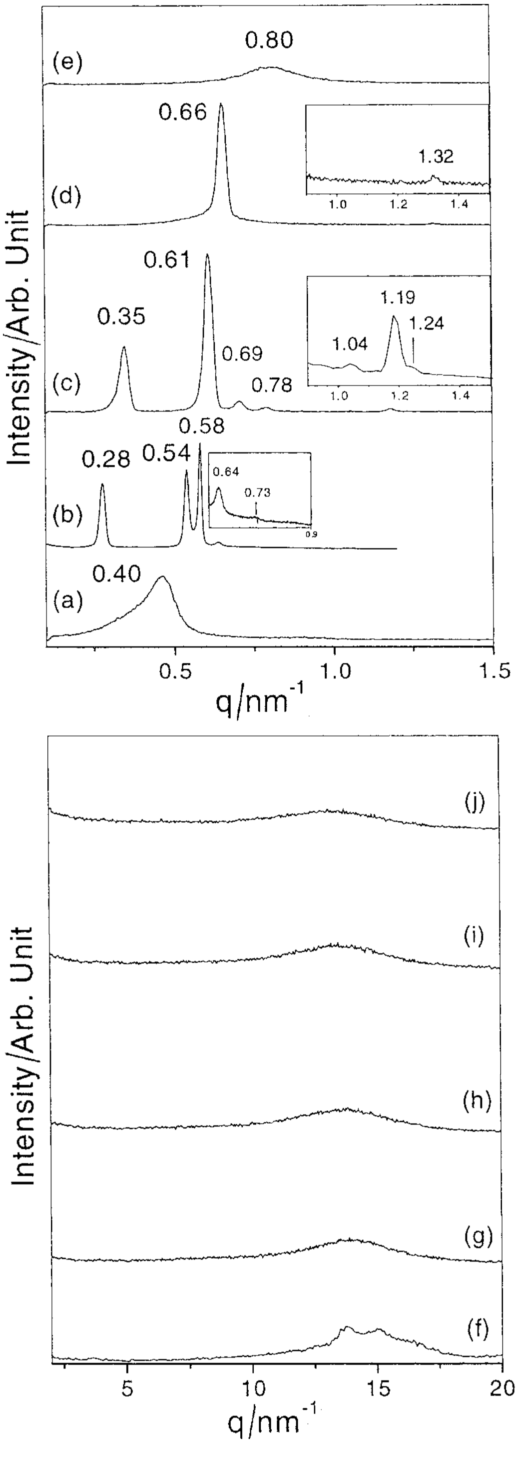

Figure 6. X-ray diffractograms measured at different temperatures plotted against $q(=4\pi \sin \theta/\lambda)$ for E-12-22-0.25. (*a*) Small angle and (*f*) wide angle XRD of lamellar crystalline phase at 70°C; (*b*) small angle and (*g*) wide angle XRD of oblique columnar phase at 108°C; (*c*) small angle and (*h*) wide angle XRD of base-centred rectangular columnar phase at 150°C; (*d*) small angle and (*i*) wide angle XRD of monolayer smectic A phase at 190°C; (*e*) small angle and (*j*) wide angle XRD of isotropic phase at 260°C.

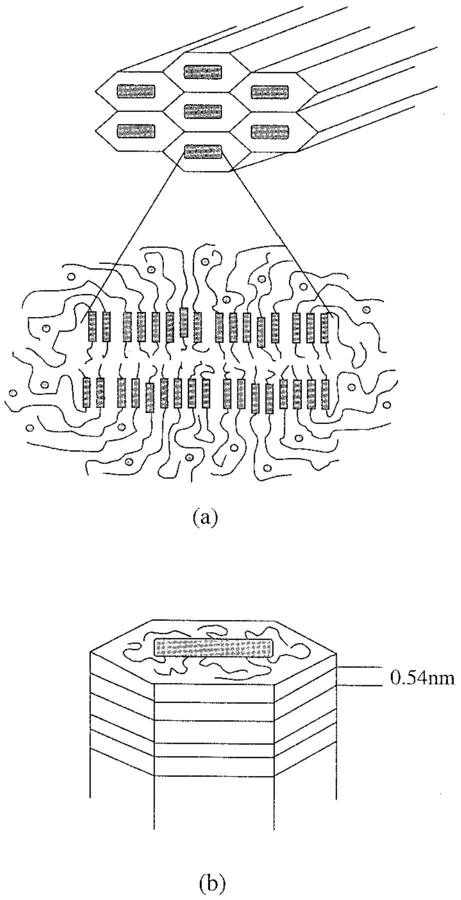

Figure 7. Schematic representation of the formation of the rectangular columnar phase of E-12-22-0.25: (*a*) top view, (*b*) tilted side view.

The lamellar structure observed in the SmC phase of E-12-22 is the most efficient packing of rods and grafted chains, similar to that of smectogens with long alkyl chains. The added lithium triflate will be selectively dissolved in the micro-separated poly(ethylene oxide) coil segments of E-12-22 through ion–dipole interaction. Lamellar ordering of rods would confine junctions within a flat interface of rods and coils with a relatively high density of grafting sites, forcing a strong stretching of the coils away from the interface; the system then becomes entropically unfavourable. Consequently, the lamellar structure of the coil–rod–coil ABC triblock molecule may break apart into a rectangular columnar phase in which coil stretching is reduced.

These complexed ABC triblock molecules have another phase transition from a columnar to a smectic phase on heating. It is a somewhat striking result from the viewpoint of phase behaviour of rod–coil molecules, because most rod–coil molecules show a lamellar to columnar phase transition with increasing temperature or with increasing coil length. The packing structure of

E-12-22-0.25 in the rectangular columnar phase is a bilayered structure, as shown in figure 7 (*a*), i.e. the inner core of the cylinder is composed of alkyl chains and two discrete aromatic cores with rectangular cross-section, while the lithium complexed poly(ethylene oxide) chains splay to fill the outer intercylinder matrix. On heating, this bilayered structure collapses, and a monolayered lamellar structure forms as shown in figure 5 (*b*). In this monolayer structure, alkyl chains, poly(ethylene oxide) chains and lithium triflate are mixed with one another. The free energy of mixing can be expressed as a sum of two contributions: enthalpy and entropy of mixing. At ambient temperature, the hydrophobic docosyl chain would not mix with hydrophilic poly(ethylene oxide) and polar lithium triflate. So the enthalpy of mixing should act unfavourably in this $\mathrm{Col_{rec}}$–SmA transition. On the other hand, this mixing generates entropies of various kinds: translational entropy of lithium triflate ion, rotational entropy (flipping) of E-12-22, and mixing entropy between docosyl chain and lithium triflate. Because the entropy finally dominates with increasing temperature, this bilayered cylinder to monolayer smectic transition may be feasible. Thus, due to the added lithium triflate, a columnar to lamellar phase transition takes place in the complexed ABC triblock molecule.

The polymorphism of E-12-22-0.25 may be explained from the viewpoint of added salt as shown in figure 8. In the crystalline state, the polar lithium triflate is selectively dissolved in microphase-segregated poly(ethylene oxide) domains as shown in figure 8 (*a*). In this state, high ion–dipolar interaction exists between the poly(ethylene oxide) and the lithium ions. So mixing enthalpy favours the microphase-separated lamellar structure. At higher temperatures, the entropic stretching penalty of poly(ethylene oxide) chains makes the system unstable so that transition to a columnar phase takes place, figure 8 (*b*). Because the added salt contacts only polar chain, the enthalpy of mixing is also favourable in this columnar phase. The $\mathrm{Col_{rec}}$ phase transforms into the SmA phase at 189°C. The added salts mix with docosyl chains as well as poly(ethylene oxide) chains as shown in figure 8 (*c*). Following the previous discussion, an increase of entropy compensates for the enthalpy increment caused by unfavourable contacts between polar salts and non-polar chains. In this mesophase, however, the contact energy between lithium triflate and rod block is so large that mixing between them can not occur. Above the isotropic temperature, the mixing entropy becomes large enough to overcome this contact energy, and homogeneous mixing (isotropization) takes place as shown in figure 8 (*d*). The isotropic state with no phase separation was confirmed by POM observation.

As mentioned earlier, isotropization temperature is greatly increased by complexation. The reason can be traced to the increase in entropy that occurs on mixing. Stabilization of the mesophase, as well as the induction of various liquid crystalline phases, results from complexation.

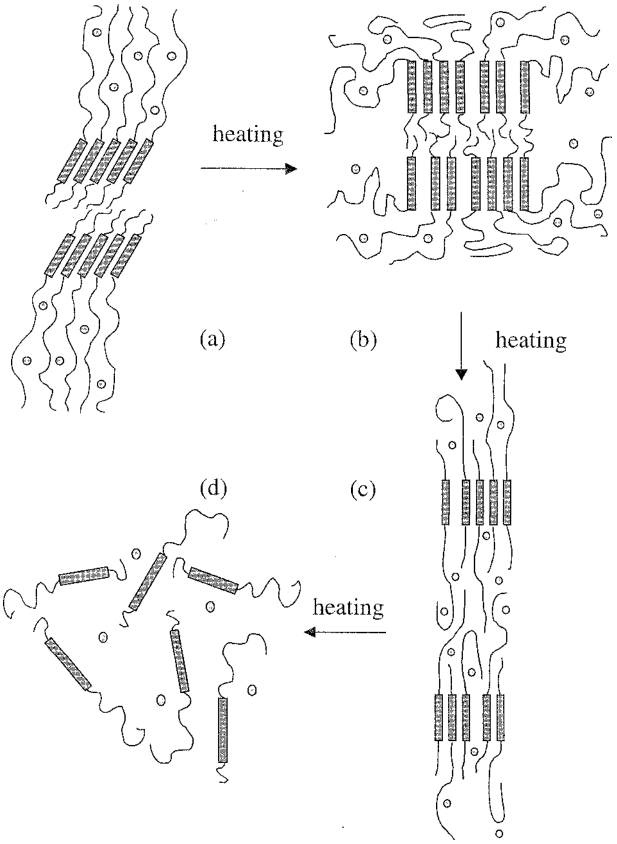

Figure 8. Schematic representation of the structures of E-12-22-0.25: (*a*) in the crystalline state, (*b*) rectangular columnar phase, (*c*) smectic A phase, (*d*) isotropic phase.

4. Conclusions

The structures of pure and lithium complexed coil–rod–coil ABC triblock molecules were characterized by observation of the optical texture with POM and by XRD. All of the experimental results led us to conclude that E-12-22 forms a SmC mesophase and E-12-22-0.25 forms $\mathrm{Col_{ob}}$, $\mathrm{Col_{rec}}$, and SmA mesophases. The phase behaviour of the rod–coil molecule is rich in features on complexation with lithium triflate. The volume fraction increment of the poly(ethylene oxide) block caused by complexation is responsible for induction of the columnar phase. Another interesting result is that complexed E-12-22 shows a columnar to lamellar (bilayer to monolayer) transition on heating. This unique phase behaviour is believed to originate from the added $\mathrm{LiCF_3SO_3}$. Stabilization of the mesophase, as well as the induction of various liquid crystalline phases is a result of complexation.

This work was supported by the '99 POSCO research fund through POSTECH and by the Center for Advanced Functional Polymers. X-ray measurements were performed at the Pohang Accelerator Laboratory (Beamline 3C2 and 4C2).

References

[1] Mao, G., and Ober, C. K., 1998, in *Handbook of Liquid Crystals*, Vol. 3, edited by D. Demus, J. Goodby, G. W. Gray, H.-W. Spiess, and V. Vill (Weinheim: Wiley-VCH), pp. 66–92.

[2] Chen, J. T., Thomas, E. L., Ober, C. K., and Mao, G.-P., 1996, *Science*, **273**, 343.

[3] Stupp, S. I., LeBonheur, V., Walker, K., Li, L. S., Huggins, K. E., Keser, M., and Amstutz, A., 1997, *Science*, **276,** 384.

[4] (*a*) Lee, M., Cho, B.-K., Kim, H., and Zin, W.-C., 1998, *Angew. Chem. int. Ed. Engl.*, **37,** 638; (*b*) Lee, M., Cho, B.-K., Kim, H., Yoon, J.-Y., and Zin, W.-C., 1998, *J. Am. chem. Soc.*, **120,** 9168; (*c*) Lee, M., Lee, D.-W., Cho, B.-K., Yoon, J.-Y., and Zin, W.-C., 1998, *J. Am. chem. Soc.*, **120,** 13 258.

[5] (*a*) Dias, F. B., Voss, J. P., Batty, S. V., Wright, P. V., and Ungar, G., 1994, *Macromol. rapid Commun.*, **15,** 961; (*b*) Percec, V., Heck, J., Johansson, G., Tomazos, D., and Ungar, G., 1994, *Macromol. Symp.*, **77,** 237.

[6] (*a*) Lee, M., Oh, N.-K., Lee, H.-K., and Zin, W.-C., 1996, *Macromolecules*, **29,** 5567; (*b*) Lee, M., Zin, W.-C., and Ji, S. H., 1996, *Bull. Kor. chem. Soc.*, **17,** 309; (*c*) Lee, M., and Cho, B.-K., 1998, *Chem. Mater.*, **10,** 1894.

[7] Lee, M., Lee, D.-W., Cho, B.-K., Kim, H., and Zin, W.-C., 1999, *Mol. Cryst. liq. Cryst.*, **330,** 351.

[8] Roe, R.-J., 2000, in *Methods of X-ray and Neutron Scattering in Polymer Science* (Oxford University Press), pp. 194–204.

[9] Helperin, A., 1990, *Macromolecules*, **23,** 2724.

[10] Malthete, J., Levelut, A. M., and Tinh, N. H., 1985, *J. Physique Lett.*, **46,** L-875.

[11] Heinrich, B., Praefcke, K., and Guillon, D., 1997, *J. mater. Chem.*, **7,** 1363.

[12] Komatsu, T., Ohta, K., Watanabe, T., Ikemoto, H., Fujimoto, T., and Yamamoto, I., 1994, *J. mater. Chem.*, **4,** 537.

[13] Zheng, H., Lai, C. K., and Swager, T. M., 1995, *Chem. Mater.*, **7,** 2067.

[14] Raja, K. S., Raghunathan, V. A., and Ramakrishnan, S., 1998, *Macromolecules*, **31,** 3807.

[15] Goldmann, D., Dietel, R., Janietz, D., Schmidt, C., and Wendorff, J. H., 1998, *Liq. Cryst.*, **24,** 407.

[16] Chandrasekhar, S., 1993, *Liq. Cryst.*, **14,** 3.

[17] Nguyen, H. T., Destrade, C., and Malthete, J., 1997, *Adv. Mater.*, **9,** 375.

[18] (*a*) Hidebrandt, F., Schroter, J. A., Tschierske, C., Festag, R., Wittenberg, M., and Wendorff, J. H., 1997, *Adv. Mater.*, **7,** 564; (*b*) Schroter, J. A., Tschierske, C., Wittenberg, M., and Wendorff, J. H., 1998, *J. Am. chem. Soc.*, **120,** 10 669; (*c*) Kolbel, M., Beyersdorff, T., Sletvold, I., Tschierske, C., Kain, J., and Diele, S., 1999, *Angew. Chem. int. Ed. Engl.*, **38,** 1077.

[19] Roe, R.-J., 2000, in *Methods of X-ray and Neutron Scattering in Polymer Science* (Oxford University Press), pp. 224–228.